LATE-PLEISTOCENE WEDGE STRUCTURES ALONG THE PATAGONIAN COAST (ARGENTINA): CHRONOLOGICAL CONSTRAINTS AND PALAEO-ENVIRONMENTAL IMPLICATIONS

ADRIANO RIBOLINI[1], MONICA BINI[1], ILARIA CONSOLONI[1], ILARIA ISOLA[2], MARTA PAPPALARDO[1], GIOVANNI ZANCHETTA[1], ENRIQUE FUCKS[3], LAURA PANZERI[4], MARCO MARTINI[4] and FILIPPO TERRASI[5]

[1]Dipartimento di Scienze della Terra, University of Pisa, Pisa, Italy
[2]Istituto di Geofisica e Vulcanologia, Pisa
[3]Facultad de Ciencias Naturales y Museo, Universidad Nacional de La Plata, La Plata, Argentina
[4]Dipartimento di Scienza dei Materiali, University of Milano Bicocca, Milano, Italy
[5]Dipartimento di Scienze Ambientali, University of Naples 2, Napoli, Italy

Rinbolini, A., Bini, M., Consolini, I., Isola, I., Pappalardo, M., Zanchetta, G., Fucks, E., Panzeri, L., Martini, M., and Terrasi, F., 2014. Late-Pleistocene wedge structures along the Patagonian coast (Argentina): chronological constraints and palaeo-environmental implications. *Geografiska Annaler: Series A, Physical Geography*, 96, 161–176. DOI:10.1111/geoa.12038

ABSTRACT. This paper investigates several wedge structures formed in continental deposits covering marine sediments deposited during MIS 5 along the central Patagonian coast of Argentina. The size and surface microtexture characteristics of the infilling sediments are consistent with a depositional environment dominated by aeolian transport. Fragments of Andean volcanic rocks (glass shards) in the wedge-fill suggest long-distance transport via a westerly component of wind direction. The wedges are interpreted as products of deep seasonal frost action in frozen ground, which produced open cracks that filled rapidly with partially non-local aeolian sediments. Many wedges cross cut carbonate crusts that formed under permafrost conditions in coastal Patagonia. The radiocarbon dating of carbonate crusts yielded an age of 25–27 kyr BP, while wedge-fill sediments are OSL dated to 14 670 ± 750 yr BP. This indicates that ground wedge formation occurred during a cold event (the Antarctic Cold Reversal period) that interrupted the permafrost degradation following the Last Glacial Maximum.

Introduction

This paper describes wedge structures in central Patagonia (latitude 46–48° S) (Fig. 1) and provides chronological constraints on wedge formation (OSL and ^{14}C dating). Late Pleistocene wedge structures have been documented in Tierra del Fuego (Coronato *et al*. 2004; Perez-Alberti *et al*. 2008), the southern limit of Patagonia (Bockheim *et al*. 2009 and references therein), and northern Patagonia (Trombotto 2002 and references therein). However, wedge features in Central Patagonia have received limited attention (e.g. Schellmann 1998), and this is the first study to report wedge structures in the area of Puerto Deseado and the coast of San Jorge Gulf.

Many proxy records indicate that the Patagonian climate experienced cold events during deglaciation from the *Last Glacial Maximum* (*LGM*; 25–27 ka BP) (Kilian and Lamy 2012 and references therein). These cold events are known to have affected Andean and piedmont areas of Patagonia, where palaeoclimatic information is abundant (Kilian and Lamy 2012), and are known to have promoted glacial advances at comparable latitudes in the western Andes (Hein *et al*. 2010; García *et al*. 2012). However, terrestrial climate proxy records are limited in the Atlantic coastal lowlands of central Patagonia, and it is relatively unknown whether areas near the modern coast of central Patagonia were sensitive to the influence of the cold periods in the Late Pleistocene.

Present day climate

The climate of Puerto Deseado and San Jorge Gulf is semi-arid, cold-temperate and characterized by frequent strong winds (Coronato *et al*. 2008; Isla and Bujalesky 2008). The climatic stations at of

© 2014 Swedish Society for Anthropology and Geography
DOI:10.1111/geoa.12038

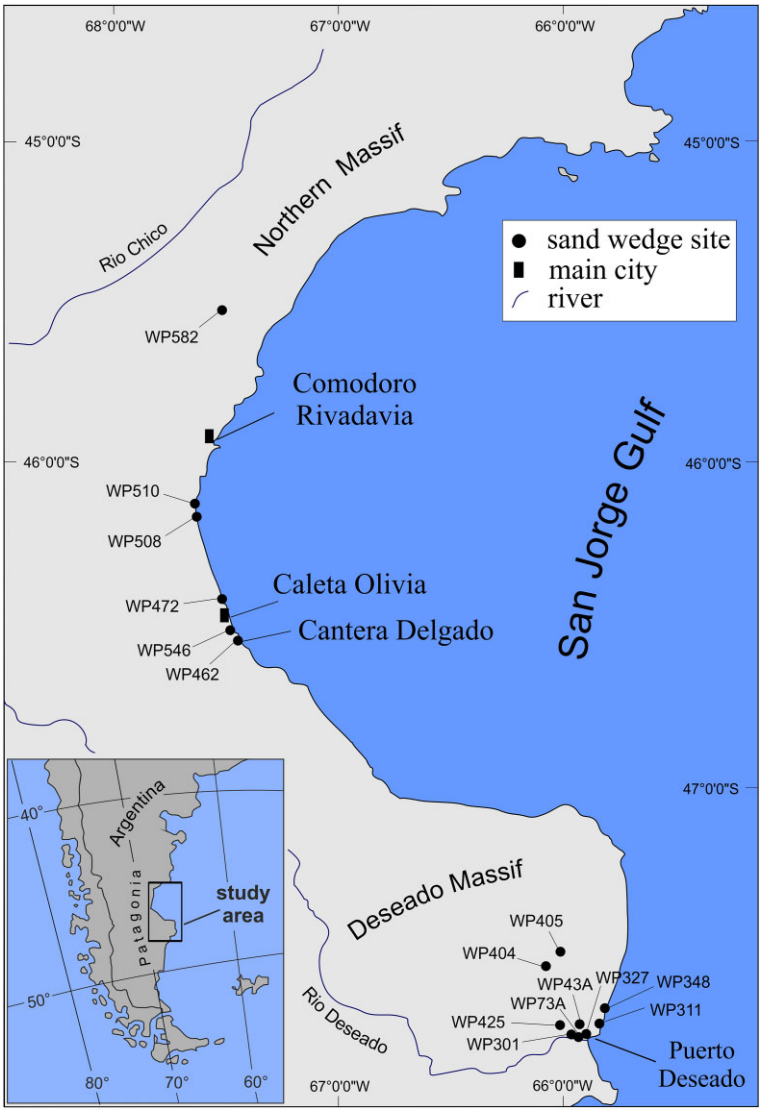

Fig. 1. Sketch map of the central Patagonian coast. Ground wedges were observed at sites indicated by a black circle/code. The codes are used in the captions of subsequent figures to indicate location.

Comodoro Rivadavia and Puerto Deseado register less than 200 mm of rainfall per year, and have yearly average air temperatures of 13.0°C and 8.2°C, respectively. Summers (January–March) are relatively hot and dry, while winter months (June–August) are characterized by fresh/cold air temperatures (7°C and 4°C, respectively) (Servicio Meteorologico Nacional-Argentina, http://www.smn.gov.ar, 5 Feb., 2014). Severe and frequent windstorms occur mainly during spring and summer (October and February, respectively), with wind speeds regularly exceeding 120 km h^{-1}. These windstorms can cause intense aeolian sediment transport, especially on unprotected soils. A strong, westerly component to wind direction is present throughout the area (del Valle *et al*. 2008; Sterk *et al*. 2012).

Geological setting

Geologically, the San Jorge Gulf is situated between the Deseado Massif to the south and the

© 2014 Swedish Society for Anthropology and Geography

Northern Massif to the north, both of which comprise Jurassic volcanic and volcano-clastic rocks (e.g. rhyolites, ignimbrites, and porphyroids). These massifs border the eastern termination of a predominantly extensional tectonic basin that trends East–West from the Andean belt to the Atlantic Ocean (Sylwan 2001).

The Pleistocene and Holocene sediments that outcrop along the Patagonian coast of San Jorge Gulf are predominantly of marine origin. The stratigraphy, palaeontology and geomorphology of these sediments have been studied widely (Schellmann and Radtke 2010; Isola *et al*. 2011; Ribolini *et al*. 2011; Zanchetta *et al*. 2012; Bini *et al*. 2013; Zanchetta *et al*. 2014 and references therein). Particularly relevant here are gravel and sandy gravel marine deposits belonging to the MIS 5 transgression (*c*. 125 kyr BP) that are unconformably overlain by Holocene marine sandy gravel deposits. The latter contains abundant fossil remains indicative of a stormy beach environment. The Pleistocene units are mantled locally by a modern aeolian cover that reaches 2 m in thickness.

Wedge structures

Sedimentary features indicative of frost wedge activity are observed along the San Jorge coast and in the area of Puerto Deseado (Fig. 1, Table 1). Morphologically, the features are regularly cuneiform to slightly irregular with wavy margins (Fig. 2a–c). The downward terminations are sharp, V-shaped, or curved upward and do not present a 'beardy' margin (Fig. 2d, e). Maximum depths are 80–130 cm (with depths of approximately 80 cm being most common), while maximum widths range between 20 and 40 cm. In some locations, the features appear as thin, irregular, sinuous veins. Polygonal networks are visible on the surface only locally due to modern soil development and active aeolian deposition. The shape of the polygons is pseudo-hexagonal, with maximum diameters approximately 1.5–2 m (Fig. 2g).

The examined wedges started to form in the base of the aeolian cover or colluvial deposits (Fig. 2). Downward development of the wedge structures resulted in cross cutting of massive horizons formed by continental depositional processes, composed of sand and sandy silt deposits with angular clasts in variable proportions. These horizons frequently contain rhizoconcretions and pedogenetic features, such as gypsum nodules and horizontal carbonate crusts, indicative of an arid depositional setting. In some instances, wedge development caused the downward displacement of host material inclusions, including fragments of carbonate crust (see also Fig. 9). No examples of deformation of sedimentary bedding were observed, nor were sorting effects observed that might reflect clast migration. Two generations of wedges are observed at some of the locations (Fig. 2f).

The best wedge structure development is observed at the Puerto Deseado and Cantera Delgado areas (Fig. 1), where wedges formed in thin colluvial and aeolian sediments that discontinuously mantled extensive Pleistocene marine sediments. A schematic geological background of both areas is reported in Fig. 3.

Table 1. Sites at which ground wedges were observed.

Site code	Latitude (S)	Longitude (W)	Elevation (m a.s.l.)
WP301	47° 45′ 03″	65° 54′ 54″	19
WP311	47° 43′ 11″	65° 50′ 28″	9
WP327	47° 45′ 18″	65° 53′ 33″	9
WP348	47° 42′ 22″	65° 49′ 57″	11
WP404	47° 30′ 50″	66° 06′ 12″	115
WP405	47° 23′ 48″	66° 03′ 52″	117
WP425	47° 44′ 38″	65° 55′ 45″	31
WP43A	47° 45′ 15″	65° 54′ 23″	12
WP73A	47° 45′ 04″	65° 53′ 39″	21
WP462	46° 33′ 31″	67° 25′ 57″	18
WP471	46° 23′ 18″	67° 32′ 51″	29
WP508	46° 08′ 36″	67° 37′ 50″	32
WP510	46° 07′ 47″	67° 37′ 49″	26
WP546	46° 28′ 05″	67° 30′ 59″	51
WP582	45° 29′ 53″	67° 35′ 52″	652

Puerto Deseado

Wedge features (Fig. 1) and polygonal cracks occurring near the surface (Fig. 2f) are observed in a section (Fig. 4) near the western margin of the Puerto Deseado village. At the base, the section comprises a fossiliferous marine gravel with sandy beds and pockets of weakly stratified sand inclined slightly seaward. The elevation of this layer (16–17 m above *high tide water*, *hTw*) is similar to that of the inner margin of the marine terraces near Puerto Deseado (Zanchetta *et al*. 2012) and is consistent with other data from the San Jorge Gulf (Rutter *et al*. 1989), allowing this deposit to be correlated with the MIS 5e highstand (*c*. 125 ka).

A sharp unconformity marks the boundary between the marine gravel described above and

© 2014 Swedish Society for Anthropology and Geography

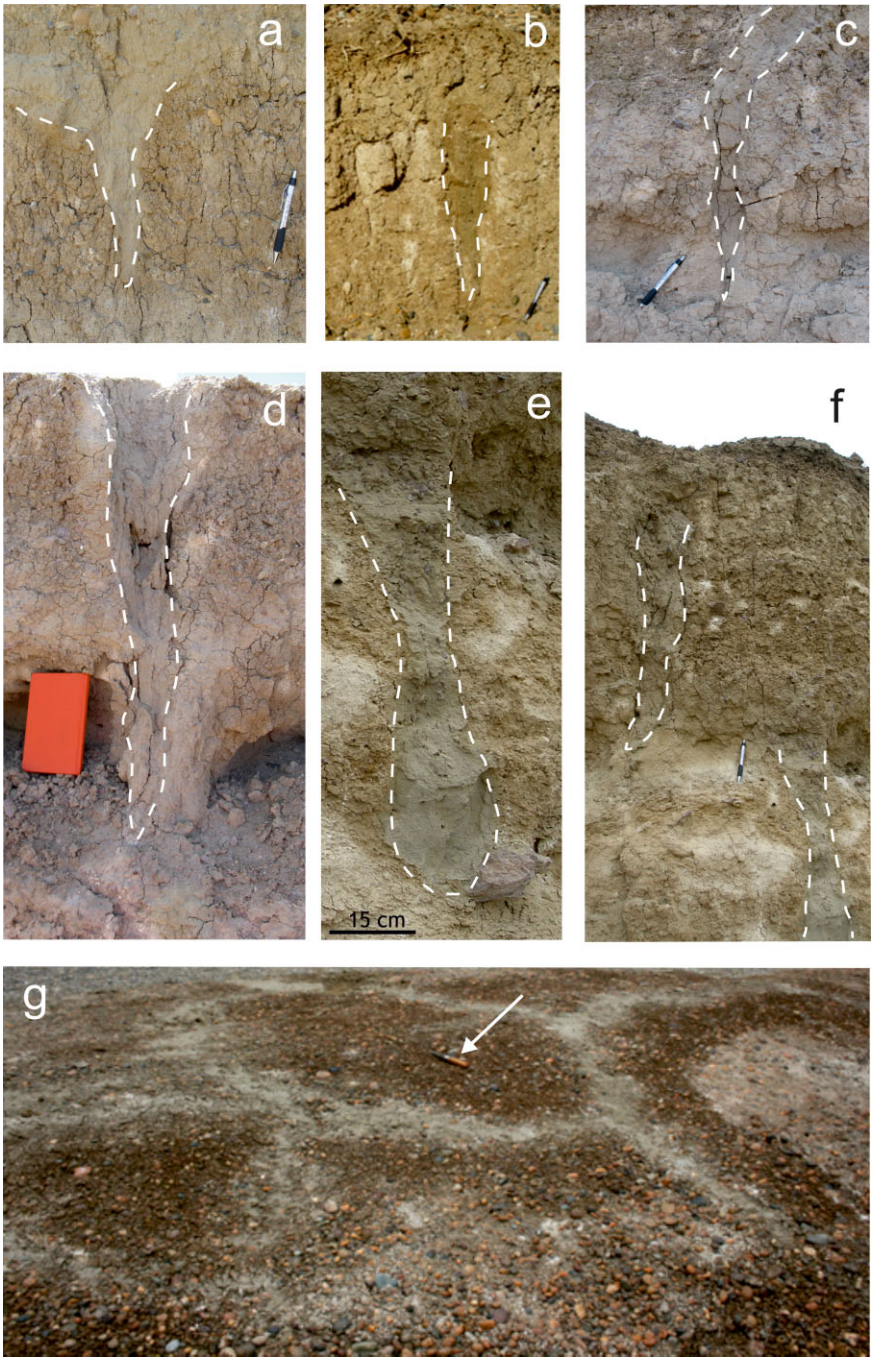

Fig. 2. Example ground wedge morphology along San Jorge Gulf and Puerto Deseado area. (a) V-shaped with undulated margins. The wedge is formed in a sandy deposit and cross cut a colluvial layer beneath (WP462). (b), (c) V-shaped with undulated and regular margins. (b) is formed in a sandy deposit and cross cuts a colluvial layer beneath (WP510); (c) is formed in a sandy deposit and cross cuts a sandy layer with interspersed angular clasts (WP546). (d) V-shaped with undulated margins and vertical dipping crack. The wedge is formed in a gravelly sandy layer (WP348). (e) Regular margin and concave upward termination. The wedge is formed in a sandy layer and cross cut unsorted sands with interspersed angular clasts (WP301). (f) Two generations of wedges formed in a sandy layer and cross cutting unsorted sands with interspersed angular clasts. The lower wedge is the same shown in (e) (WP301). (g) Polygonal network (note the knife for scale) (WP327).

© 2014 Swedish Society for Anthropology and Geography

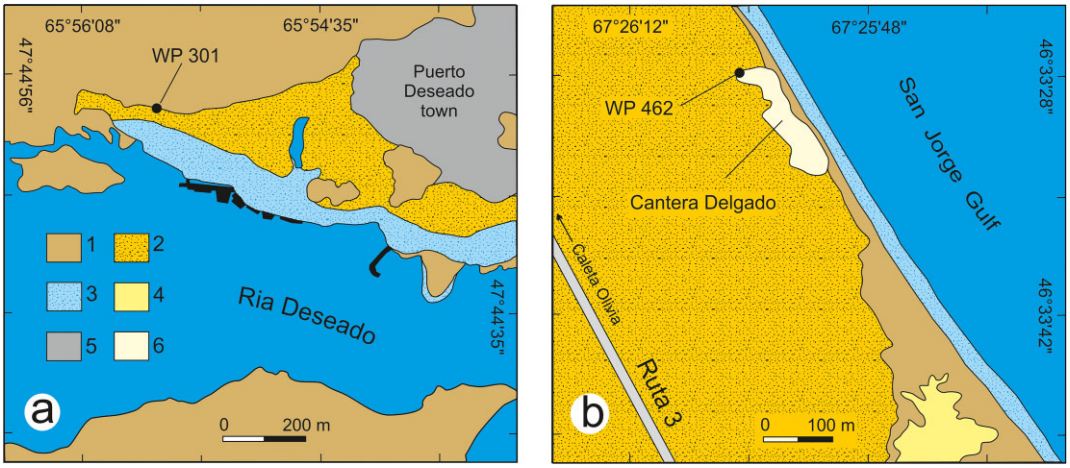

Fig. 3. Simplified geological maps of the Puerto Deseado (a) and Cantera Delgado (b) areas. 1: bedrock (volcanic rocks); 2: Pleistocene marine deposits (MIS 5e); 3: Holocene marine deposits; 4: Holocene aeolian cover; 5: urbanized area; 6: quarry.

a continental lithostratigraphic unit (17–17.6 m hTw) composed of massive silts and fine sands at the base and then by silt and clay with centimetre-scale horizontal layers of pedogenetic carbonate crust higher (Bk horizon). Considering the proximity to the fluvial valley of Río Deseado (Fig. 1), it is feasible that these sediments were deposited on a fluvial plain.

The unit above is conformably overlain by a matrix-supported deposit of angular bedrock fragments sustained by an unsorted coarse sand (17.6–18.2 m hTw). Subaerial slope processes (slope debris) can be invoked for the formation of this deposit. A poorly sorted, coarse-skewed and leptokurtic grey to pale-yellow fine-sand layer in the middle of the section, from 18.2 to 18.6 m hTw (WP301A in Fig. 5), is consistent with a partly reworked aeolian deposit. This unit contains visible wedge features (Fig. 4, see also Fig. 2e).

Vertical wedge development is from 80 to 120 cm, and the wedges feature clear lateral margins and sharp, V-shaped or curved-upward terminations. The upper limits of the wedges are coincident with, or very close to, the upper limit of the sandy layer in which they were hosted. The wedge infill deposits feature a massive structure without vertical cracks (Fig. 2e) and are composed of fine grain-sized sand, moderately sorted, with a symmetrical skewness and a mesokurtic kurtosis (WP301G, WP301H; Fig. 5).

Above the wedge-containing layer is a deposit composed of angular fragments of bedrock sustained by an unsorted coarse sand (18.6–19.4 m hTw). This unit is similar to that described in the 17.6–18.2 m hTw interval, and it can be interpreted analogously as slope debris involved in short and moderate transport.

The sandy layer in the 19.4–19.6 m hTw interval is cut by a second generation of wedge features (Fig. 2f) that, with respect to the first generation (see also Fig. 2e), are more numerous and present a regular lateral spacing of 2–3 m (Fig. 6). Vertical wedge dimensions range between 80 and 130 cm, with maximum widths of approximately 30 cm. The wedge margins are sharp and gently undulated, and the terminations are prevalently V-shaped. The tops of the wedges are situated near the base of the sandy layer described at 19.4–19.6 m hTw. Locally, vertical to steeply dipping cracks affect the wedges, dividing the sandy infillings into tabular elements (Fig. 6). The grain size corresponds to fine sand, moderately well sorted, with a symmetrical skewness and a mesokurtic kurtosis (WP301F, WP301K, WO301J; Fig. 5).

The succession terminates with a dark brown Ah soil horizon, covered by aeolian and colluvial sands associated with present-day soil degradation.

SEM analysis to identify surface microtextures and therefore specific depositional environment were focused on the morphological characteristics of quartz grains from wedge infillings and the sandy host sediments. Wedge-fill grains (first and second generation) are subrounded (Fig. 7a) and exhibit low-relief surfaces with rounded

© 2014 Swedish Society for Anthropology and Geography

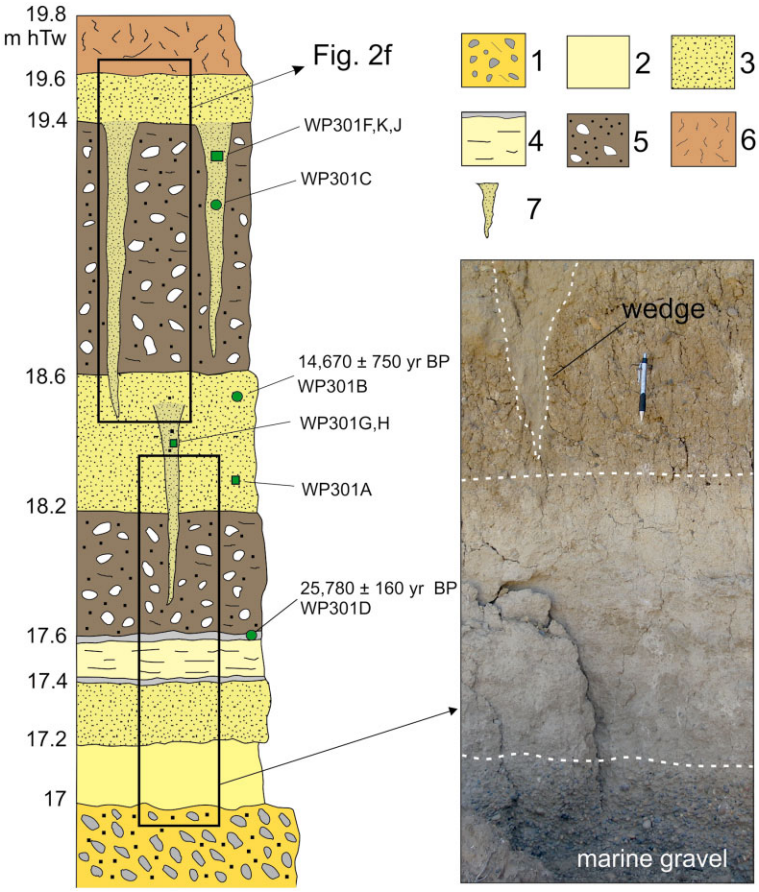

Fig. 4. The Puerto Deseado schematic section (WP301) where several wedges were observed. 1: Clinostratified gravel with marine fossils; 2: massive and cohesive silt; 3: sand; 4: silt and clay with horizons of pedogenetic carbonate crusts (in gray); 5: unsorted sand with interspersed angular clasts; 6: soil, Ah horizon; 7: wedge. Elevations are above the high tide water (hTw).

corners (Fig. 7b), dish-shaped depressions (upturned plates) (Fig. 7c), silica precipitation and conchoidal fractures (Fig. 7d). Locally, crescentic, straight and arc-shaped steps, small scratches and 'breakage-block' features are observed (Fig. 7e, f). Volcanic glass shards are also observed in the wedge-fill, and these exhibit a quenching morphology that varies from pomiceous (oval and stretched vesicles) to bubble wall (Fig. 7f, g), both of which are indicative of explosive eruptions with high fragmentation and dispersion. Additionally, some glass shard textures indicate shattering processes (Fig. 7h) that may be related to magma having made contact with glacier ice above. The rapid cooling of magma inhibited the development of vesicles and caused fractures due to thermal contraction.

Cantera Delgado

In the area of Caleta Olivia, several wedge features are found in sections along the coast. Wedges and other stratigraphic horizons are well preserved in a section situated a few kilometres south of Caleta Olivia, inside the quarry called Cantera Delgado (Schellmann 1998; Fig. 3b and 8).

At the base, the fossil-rich succession of cross-bedded sand, containing decimetres-thick layers of gravel with sandy pockets, represents a Pleistocene marine unit and rests on a shore platform carved in volcanic bedrock. Electron spin resonance ages of 95 and 75 ka BP have been obtained from fossils collected from the top of this unit (Schellmann 1998). Accordingly, MIS 5e (*c*. 125 Ka BP) is

© 2014 Swedish Society for Anthropology and Geography

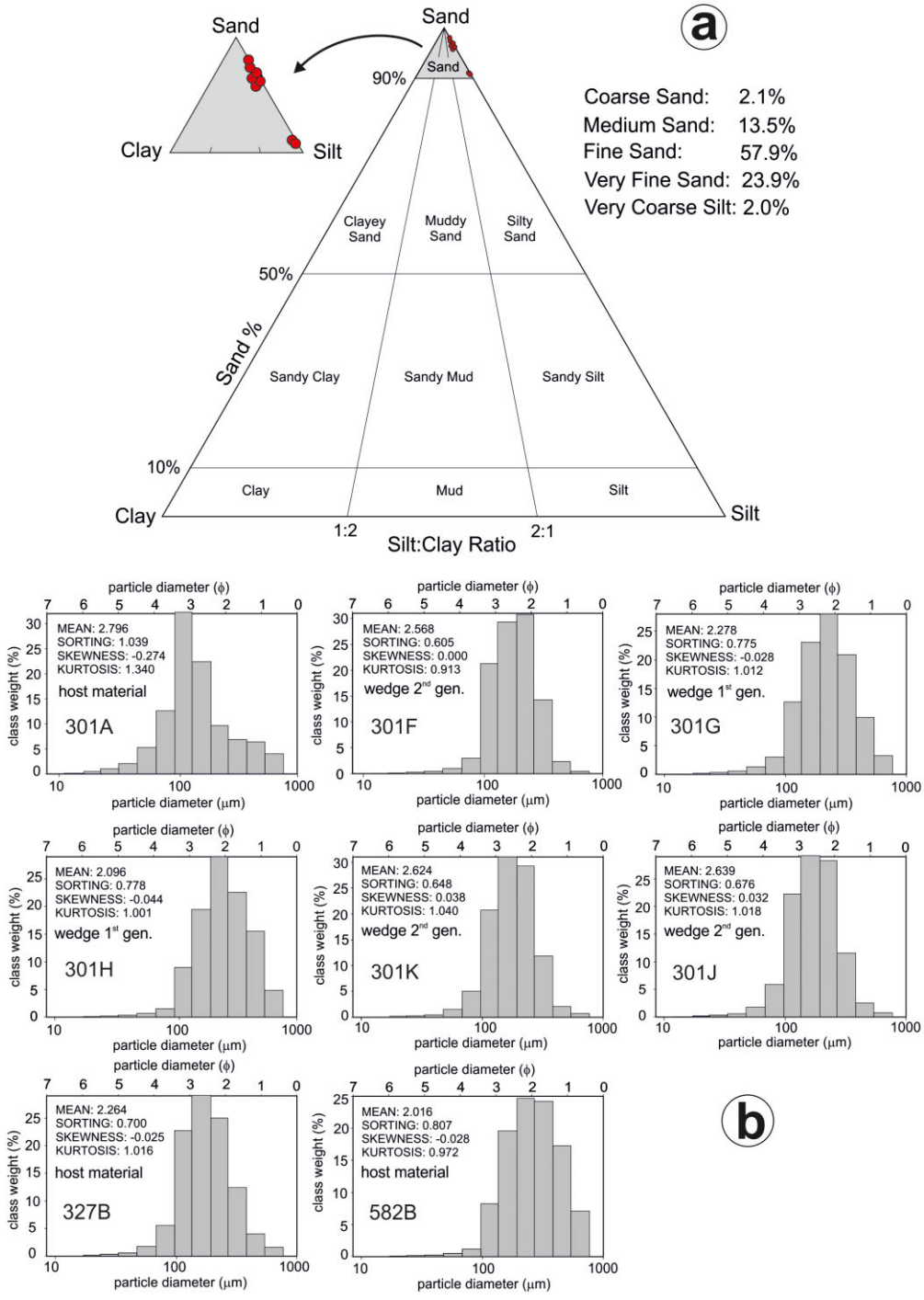

Fig. 5. Grain size analyses. (a) Clay–silt–sand triangular diagram, showing the grain size composition of the samples. An enlargement of the sand field is shown (upper left corner). (b) Grain size distribution of sample 301A obtained from host sediment at WP301; the other distributions are for samples from the wedge infillings. Statistics obtained using GRADISTAT (Blott and Pye 2001).

© 2014 Swedish Society for Anthropology and Geography

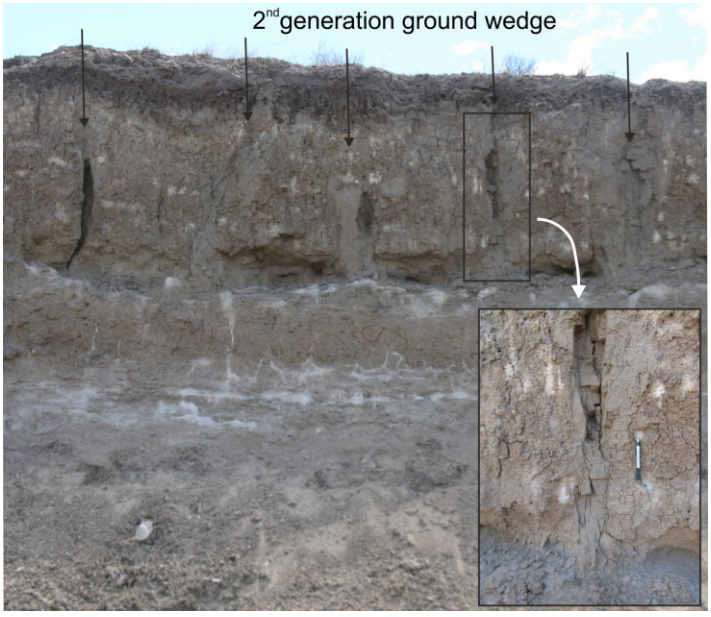

Fig. 6. Ground wedges of second generation in the Puerto Deseado section (WP327).

considered feasible for the transgression phase that built this marine unit to a height of approximately 15 m hTw (Fig. 8).

The continental deposit resting on the MIS 5e gravel is composed of silty sands with dispersed pebbles and features horizontal pedogenetic carbonate crusts of 8–10 cm in thickness (Fig. 9). The wedge features visible in this layer are characterized by vertical development of 80–100 cm and maximum widths of 10–20 cm. The margins are undulated and the terminations are sharp and V-shaped. Although grain size was not determined analytically, visually, the infilling is sandy and finer than the hosting material. Wedge growth has cross cut the pedogenetic crust, causing a downward translation of some fragments of carbonate (Fig. 9).

The series continues upward with grey massive sands containing rhizoconcretions and pedogenetic carbonate nodules. This unit corresponds to aeolian sand cover. An Ah soil horizon terminates the succession, covered by loose deposits due to the present soil degradation caused by grazing and quarry activity.

Chronology

In the Puerto Deseado section, radiocarbon dating of the pedogenetic carbonate crust at 200 cm depth (Fig. 4) yielded an age of 25 780 ± 160 yr BP (30 404–30 774 cal yr BP; WP301D). Dating of a crust cross cut by a sand wedge in the Cantera Delgado section yielded a similar age of 27 900 ± 320 yr BP (31 594–32 497 cal yr BP; WP462B; Figs 8 and 9, and Table 2). In both cases, the crust ages provide a maximum age of 25–27 ka BP for the timing of wedge development.

Radiocarbon ages obtained from pedogenetic carbonates do not necessarily represent the true age of formation if there has been incorporation of old limestone (e.g. Chen and Polach 1986) or if ^{14}C activity in soil-respired CO_2 was lower compared with atmospheric CO_2 (Wang *et al*. 1994). In addition, redissolution and reprecipitation of calcite is possible after burial. The incorporation of old limestone or lower $^{14}CO_2$ activities would make the radiocarbon age appear older than the true age, whereas redissolution/reprecipitation processes may produce younger ages. Assuming no redissolution processes and that the incorporation of old limestone is improbable (due to the non-carbonate nature of the substrate host deposits), the ages of the pedogenic carbonates (Table 2) can be considered maximum ages of the samples.

In the Puerto Deseado section, samples for OSL dating were collected from the infill of a second-generation wedge and from the sandy host

© 2014 Swedish Society for Anthropology and Geography

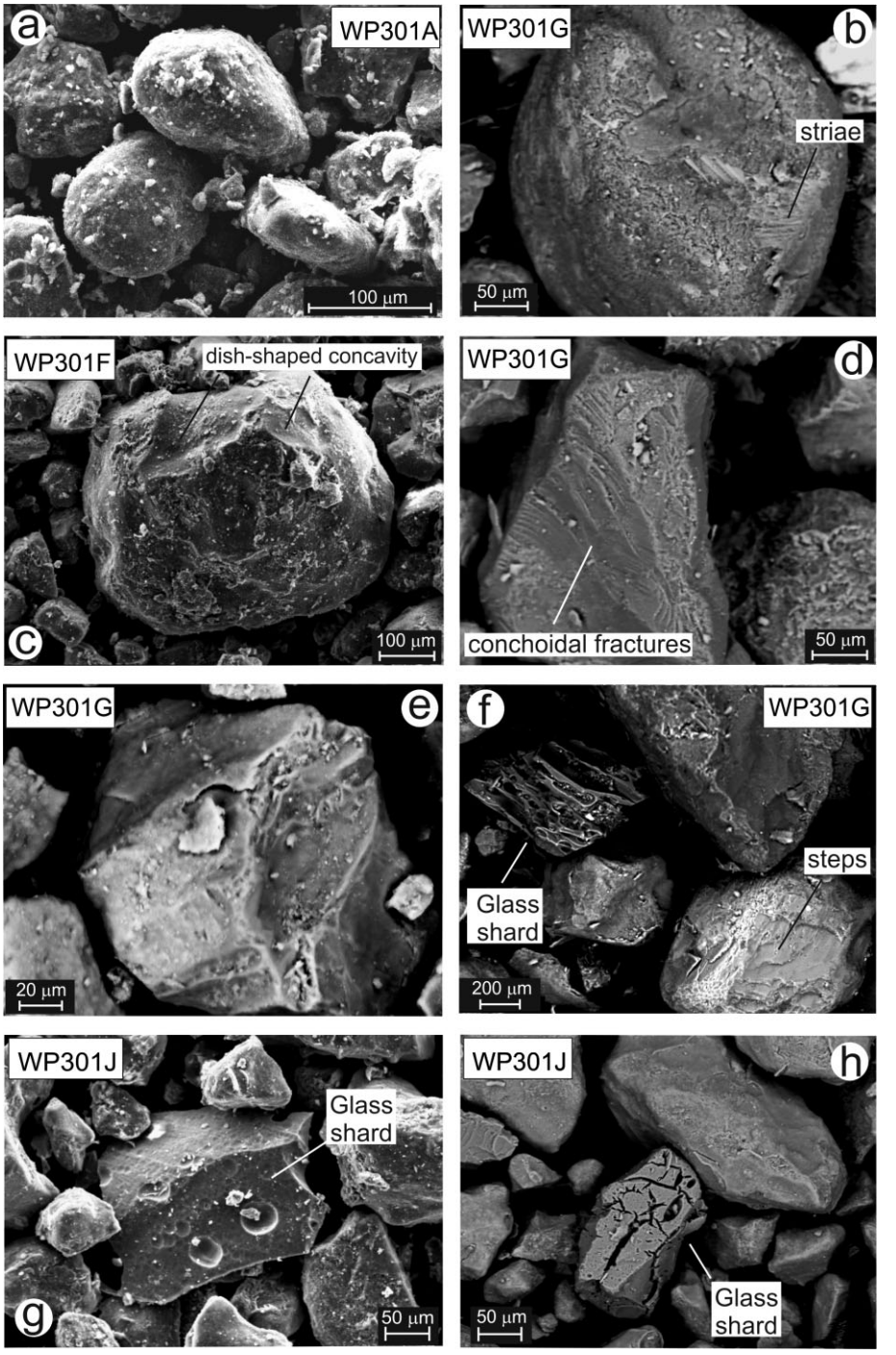

Fig. 7. SEM imagines illustrating the morphology of quartz grains of the ground wedge infillings. (a) Subrounded grains. (b) Subrounded grain with scratches and low relief surface locally plastered by silica precipitation. (c) Subrounded grain, with dish-shaped concavities and silica precipitations. (d) Conchoidal fractures and breakage block features. (e) Subrounded grain with crescent steps. Pumiceous glass-shard with stretched vesicles. (f) Irregular grain with a breakage block feature. (g) Shattered glass shard. (h) Bubble-wall glass shard.

© 2014 Swedish Society for Anthropology and Geography

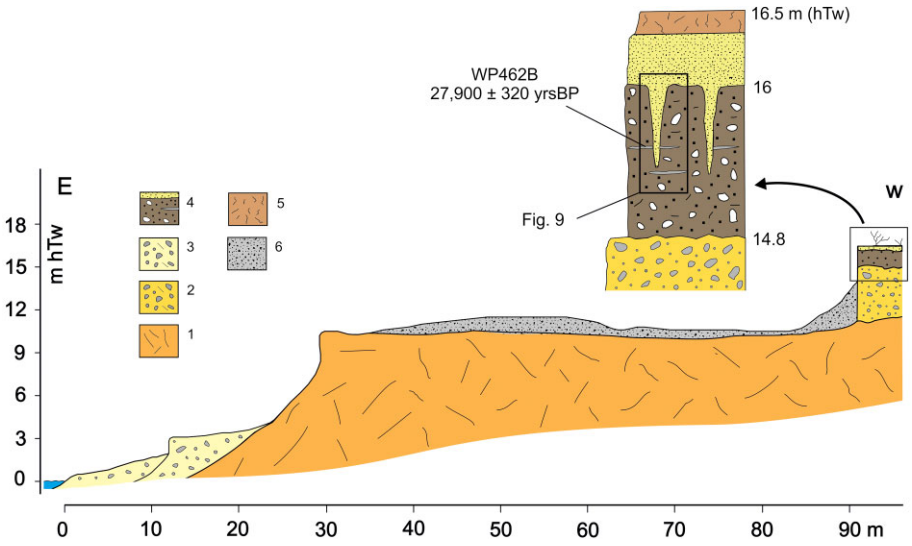

Fig. 8. The Cantera Delgado section (WP461) (not to scale). 1: bedrock; 2: Pleistocene marine deposits; 3: Holocene marine deposits; 4: Holocene continental deposits; 5: soil; 6: quarry waste deposit. See the text for a detailed litostratigraphic description. The radiocarbon age of the pedogenetic carbonate crust is indicated. An enlargement of the sand wedge is shown in Fig. 9. Elevations are above the high tide water (hTw).

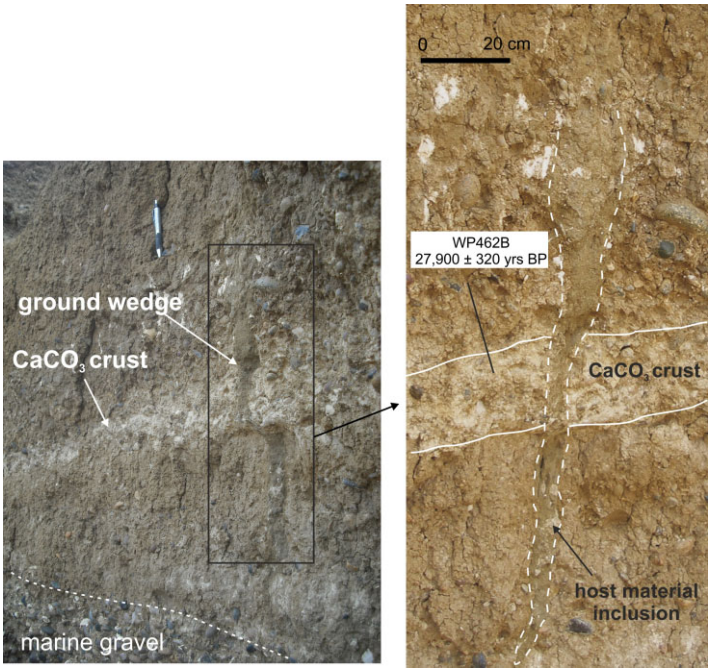

Fig. 9. Detail of sand wedge from Fig. 8. Host material (pedogenetic crust) has moved downward as the wedge has developed. The crust yielded an OSL age of 27,900 ± 320 yr BP.

© 2014 Swedish Society for Anthropology and Geography

Table 2. Radiocarbon ages obtained for this study. Ages were measured at the CIRCE laboratory of Caserta (Italy) (Terrasi *et al*. 2008). Calibration has been performed using INTCAL09.14c data set in CALIB 6 (Reimer *et al*. 2009).

Sample	Site code	^{14}C yr BP measured ages	^{14}C cal yr BP (±1σ)	Species or material
DSH1964	WP 301D	25 780 ± 160	30 404–30 774	Pedogenic carbonate
DSH4033	WP 462B	27 900 ± 320	31 594–32 497	Pedogenic carbonate

Table 3. Summary data for OSL ages obtained for this study. See supplementary information for details on the OSL procedure.

Sample	Water content (%)	D_e (Gy)	ppm U	ppm Th	ppm ^{40}K	Dose rate (mGy/a)	Age (a)
WP301B	23 ± 1	33 ± 2	1.91 ± 0.09	6.02 ± 0.30	1.91 ± 0.06	2.25 ± 0.07	14 670 ± 750
WP301C	24 ± 1		1.44 ± 0.07	4.54 ± 0.20	1.91 ± 0.06	2.14 ± 0.06	not datable

sediment at 115–160 cm depth (Fig. 4). The OSL age determination procedure is reported in the supplementary material (Fig. S1). The results show that the first generation of wedges formed in a sandy layer that yielded an OSL age of 14 670 ± 750 yr BP (Table 3). Taking into account the uncertainties of the OSL age and accepting that frost cracking occurred subsequent to or syngenetically with host sediment deposition, an age of *c*. 14–15 ka BP is proposed for the wedge formation.

Discussion

Wedge formation

The wedge features studied along the San Jorge Gulf coast and in the Puerto Deseado area exhibited maximum vertical dimensions of approximately 1.5 m and were closely spaced (2–3 m). The polygonal networks on the surface were of similar dimensions (maximum diameters approximately 2 m). The infillings are consistently massive, without any vertical or steep laminations. Analyses of infilling sediments indicated fine sand (125–200 mm, 2–3 ϕ), moderately sorted, with a symmetrical skewness and a mesokurtic kurtosis. These characteristics are consistent with a depositional environment dominated by aeolian transport and are consistent with grain-size curves for similar sediments in Patagonia (Smith *et al*. 2003; Zarate 2003). The difference in grain size between infillings and enclosing sediments is in many cases visually evident (e.g. Cantera Delgado), but is weak and limited in the degree of sorting and skewness for wedges formed in aeolian covers (e.g. Puerto Deseado).

Quartz grain microtextures, such as sub-rounded shapes, dish-shape concavities, rounded edges and polished surfaces, point to an aeolian depositional environment (Whalley and Langway 1980; Sun *et al*. 2006). Some grain characteristics may also be interpreted as the effect of cryogenic weathering (i.e. conchoidal and breakage fractures) (Wright *et al*. 1998; Sun *et al*. 1999; Frütsch 2011; Woronko and Hoch 2011). The existence of fragments of Andean volcanic rocks (glass shards) in the wedge infillings suggests long-distance transport (more than 650 km) in an eastward direction.

These data indicate that the wedge features reflect deep, seasonal frost action, with open cracks in the surface of a frozen ground that rapidly filled with sediments of not exclusively local derivation. The alternative process of desiccation cracking can be excluded because this type of cracking is uncommon in sand-sized materials (Allen 1982), such as the sandy and gravelly sandy layers that host the observed wedges. Furthermore, wedge widths and depths observed are greater than those normally exhibited by desiccation cracking, which are generally less than 0.05 m and 0.25 m, respectively (Allen 1982).

Climatic and environmental implications

A frost-wedge origin of the features means that the radiocarbon and OSL ages (Tables 2 and 3) indicate climatic conditions in the central Patagonian coast between 30 and 15 ka BP that were consistent with seasonally frozen ground. Previously, indurated carbonate crusts (*caliche*) along the Patagonian coast that are similar to those in Deseado and Delgado sections have been attributed to an arid and perennially frozen environment (permafrost) (del Valle and Beltramone 1987; Vogt and del Valle 1994).

© 2014 Swedish Society for Anthropology and Geography

Our study therefore indicates that a period of ground wedge formation most likely occurred at the end of a period of permafrost degradation following the LGM, when deep seasonal frost became the exclusive action affecting the subsurface under warmer conditions (e.g. French *et al*. 2009). It is possible that frost cracking of both the seasonally frozen layer and the perennially frozen sediment beneath may have occurred in some locations, but evidence for wedge formation under permafrost conditions is currently lacking.

Terrestrial and oceanic proxy records for the southern hemisphere indicate that the deglaciation following the LGM (23–25 Ka BP) experienced an Antarctic pattern, which is characterized by a temperature plateau or a reversal trend in the 12.5–15 ka BP interval (*Antarctic cold reversal*, *ACR*) (Fig. 10). Cold temperatures and pronounced aridity during the ACR period are demonstrated by glacial advances (Kaplan *et al*. 2011; García *et al*. 2012), desiccation of lakes (i.e. Lago Cardiel) (Stine and Stine 1990), and pollen records indicative of a treeless, and open (tundra-like) landscape dominated by eurythermal herbs and shrubs (Markgraf and Huber 2010). In this respect, our results support the hypothesis that the present coastal environment of the Central Patagonia, similar to more internal regions, also reacted to the lower ACR temperatures and higher aridity, promoting deep seasonal frost cracks that filled with aeolian sediments. The coastal area would therefore have been characterized by conditions conducive to frost cracking (Svensson 1988; Burn 1990), including scarce vegetation, limited persistence of the seasonal snow cover, and a mean annual air temperature at least 10°C lower than today. These environmental conditions are consistent with a continental lowland hundreds of kilometres inland from the coast, as the studied area was during the Late Pleistocene. Furthermore, the presence of volcanic glass shards of Andean provenance in the wedge fill of volcanic glass shards of Andean provenance demonstrates the influence on the Patagonian coast of the South Western Wind atmospheric current, which, during the ACR, promoted long-distance transport of sediment. More specifically, the radiocarbon-dated Reclús eruption at 14 900 yr BP (Haberzettl *et al*. 2009) may be the source of the volcanic fragments in the studied sand wedges, although further work using micro-analytical techniques would be required to confirm this hypothesis.

Conclusion

Ground wedge structures in the continental deposits that cover MIS 5 marine sediments in the region of Puerto Deseado and the San Jorge Gulf are indicative of frost cracking in seasonally frozen ground. Sedimentological evidence has verified this thermal condition at several locations along the Argentinean coast of Patagonia between latitudes 46 and 48°S and complements existing evidence of even colder ground thermal conditions (i.e. permafrost) from locations further south and in Tierra del Fuego (Coronato *et al*. 2004; Bockheim *et al*. 2009).

Furthermore, ages of carbonate crusts and ground wedge formation provide evidence of long-term climatic warming that saw deep seasonal frost becoming the dominant process at the end of a period of permafrost degradation beginning after the LGM.

Geological and geomorphological evidence from the Patagonian coast region has traditionally been exploited to provide palaeoenvironmental archives of sea level oscillations and the oceanic conditions (i.e. temperature and salinity) registered by marine fauna (e.g. Schellmann and Radtke 2010). In contrast, published evidence for climate-driven continental processes is less common, especially in the context of the Late Pleistocene. The evidence presented in this paper that documents the ACR-related decrease/reversal in temperature following the LGM is therefore unusual. Furthermore, it indicates the potential to improve land-based records of Late Pleistocene climate and environmental changes in this region using geomorphological approaches. In particular, the grain-size composition of wedge infill indicates relatively dry aeolian processes and a westerly component in the dominant winds that allowed the products of Late Glacial eruptions to reach the present Patagonian coast.

Acknowledgements

Discussions with Prof. Emeritus Hughes French greatly improved the manuscript and we thank Prof. A. Coronato and Prof. E. Kolstrup for their insightful reviews. We would also like to acknowledge Prof. D. Swift for useful suggestions and final review. The professional editing services of the American Journal Experts provided an English revision of the manuscript. This work was made possible thanks to the funding of the University of Pisa (Progetto Ateneo 2007, Leader G. Zanchetta) and MIUR (PRIN2008, Leader G. Zanchetta). We thank J. Cause and the CADACE no-profit

© 2014 Swedish Society for Anthropology and Geography

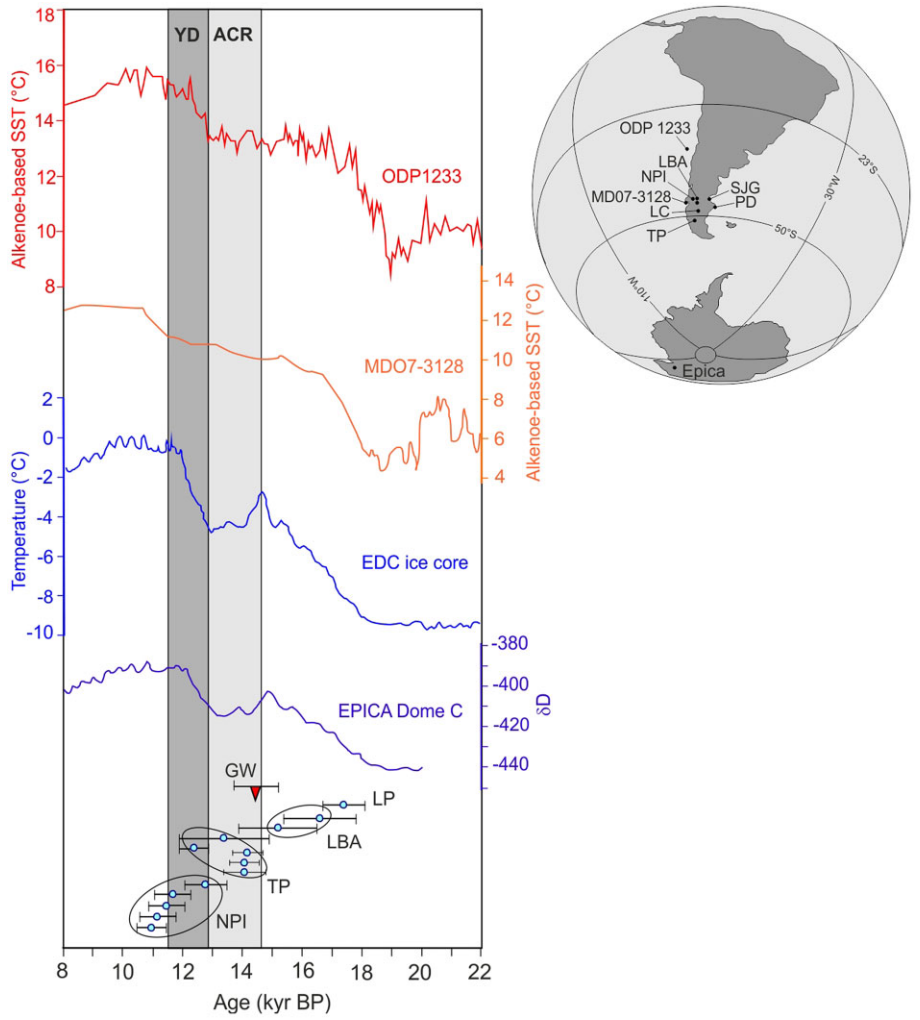

Fig. 10. Sand wedge age (red triangle, SW) (this work) in the context of palaeoclimate information for Patagonia. Alkenone sea surface temperature records are from the South Pacific cores ODP 1233 and MD07-3128. Antarctic surface temperature changes (EDC) (deviation from mean of the last millennium; Jouzel *et al*. 2007) plotted on the Lemieux-Dudon time-scale (Lemieux-Dudon *et al*. 2010). Changes of the isotopic fractionation of hydrogen in water (ice) measured at the ice core EPICA Dome C (Antarctic) (Stenni *et al*. 2004). Surface exposure ages of glaciers advances (blue points with uncertainty bar). LP: Lago Pueyrredon (Hein *et al*. 2010); LBA: Lago Buenos Aires (Hein *et al*. 2010); TP: Torres del Paine (Fogwill and Kubick 2005; Moreno *et al*. 2009; García *et al*. 2012); NPI: North Patagonian Icefield (West to the Lago Buenos Aires) (Glasser *et al*. 2012). Ages were calculated with the Dunai time-dependent scaling scheme, adopting the isotopic production rate tested for South America (Putnam *et al*. 2010). YD = Younger Dryas, ACR = Antarctic Cold Reversal. In the map: SJG = St Jorge Gulf, PD = Puerto Deseado, LC = Lago Cardiel.

organization for providing logistical support to the field campaign.

Adriano Ribolini, Monica Bini, Ilaria Consoloni, Ilaria Isola, Marta Pappalardo, Giovanni Zanchetta, Dipartimento di Scienze della Terra, University of Pisa, Pisa, Italy
E-mail: ribolini@dst.unipi.it

Enrique Fucks Facultad de Ciencias Naturales y Museo, Universidad Nacional de La Plata, Paseo del Bosque s/n, B1900FWA, La Plata, Argentina

Marco Martini, Laura Panzeri, Dipartimento di Scienza dei Materiali, University of Milano Bicocca, Via Roberto Cozzi 53, 20125 Milano, Italy

© 2014 Swedish Society for Anthropology and Geography

Filippo Terrasi Dipartimento di Scienze Ambientali, University of Naples 2, Via Vivaldi 43, 81100 Caserta, Italy

References

Allen, J.R.L., 1982. *Sedimentary Structures: their Character and Physical Basis*. Developments in Sedimentology, 30B. Elsevier, Amsterdam, 663 p.

Bini, M., Consoloni, I., Isola, I., Pappalardo, M., Ragaini, L., Ribolini, A. and Zanchetta, G., 2013. Markers of palaeo sea-level in rocky coasts of Patagonia (Argentina). *Rendiconti Online della Società Geologica Italiana*, 20, 10–14.

Blott, S.J. and Pye, K., 2001. GRADISTAT: a grain size distribution and statistics package for the analysis of unconsolidated sediments. *Earth Surface Processes and Landforms*, 26, 1237–1248.

Bockheim, J., Coronato, A., Rabassa, J., Ercolano, B. and Ponce, J., 2009. Relict sand wedges in southern Patagonia and their stratigraphic and paleo-environmental significance. *Quaternary Science Reviews*, 28, 1188–1199.

Burn, C.R., 1990. Implications for palaeoenvironmental reconstruction of recent ice-wedge development at Mayo, Yukon Territory. *Permafrost and Periglacial Processes*, 1, 3–14.

Chen, Y. and Polach, H., 1986. Validity of 14C ages of carbonate sediments. *Radiocarbon*, 28, 464–472.

Coronato, A., Bujalesky, G., Pérez Alberti, A. and Rabassa, J., 2004. Evidencias criogénicas fósiles en depósitos marinos interglaciarios de Tierra del Fuego, Argentina. *X Reunión Argentina de Sedimentología, Acta de Resúmenes*, San Luis, Argentina, 48–49.

Coronato, M.J., Coronato, F., Mazzoni, E. and Vásquez, M., 2008. The physical geography of Patagonia and Tierra del Fuego. In: Rabassa, J. (ed.), *Late Cenozoic of Patagonia and Tierra del Fuego*. Elsevier, Amsterdam. 13–55.

del Valle, H. and Beltramone, C., 1987. Morfología de las acumulaciones calcáreas en algunos paleosuelos de Patagonia Oriental (Chubut). *Ciencia del Suelo*, 5, 77–87.

del Valle, H.F., Rostagno, C.M., Coronato, F.R., Bouza, P.J. and Blanco, P.D., 2008. Sand dune activity in northeastern Patagonia. *Journal of Arid Environments*, 72, 411–422.

Fogwill, C.J. and Kubick, P.W., 2005. Glacial stage spanning the Antarctic cold reversal in Torres del Paine (51ıS), Chile, based on preliminary cosmogenic exposure ages. *Geografiska Annaler: Series A, Physical Geography*, 87, 403–408.

French, H., Demitroff M. and Newell, W.L., 2009. Past permafrost on the mid-Atlantic coastal plain, eastern United States. *Permafrost and Periglacial Processes*, 20, 285–294.

Frütsch, F., 2011. *Quartz grain weathering in a periglacial environment: indications from SEM and TEM studies using single grain features*. Master thesis, Fachbereich Geowissenschaften, Freie Universität Berlin, Germany.

García, J.L., Kaplan, M.R., Hall, B.L., Schaefer, J.M., Vega, R.M., Schwartz, R. and Finkel, R., 2012. Glacier expansion in southern Patagonia throughout the Antarctic cold reversal. *Geology*, 40, 859–862.

Glasser, F.G., Harrison, S., Schnabel, C., Fabel, D. and Jansson, K.N., 2012. Younger Dryas and early Holocene age glacier advances in Patagonia. *Quaternary Science Reviews*, 58, 7–17.

Haberzettl, T., Anselmetti, F.S., Bowen, S.W., Fey, M., Mayr, C., Zolitschka, B., Ariztegui, D., Mauz, B., Ohlendorf, C., Kastner, S., Lücke, A., Schäbitz, F. and Wille, M., 2009. Late Pleistocene dust deposition in the Patagonian steppe e extending and refining the paleoenvironmental and tephrochronological record from Laguna Potrok Aike back to 55 ka. *Quaternary Science Reviews*, 28 (25–26), 2927–2939.

Hein, A.S., Hulton, N.R.J., Dunai, T.J., Sugden, D.E, Kaplan, M.R. and Xu, S., 2010. The chronology of the Last Glacial Maximum and deglacial events in central Argentine Patagonia. *Quaternary Science Reviews*, 29, 1212–1227.

Isla, F.I. and Bujalesky, G.G., 2008. Coastal geology and morphology of Patagonia and the Fuegian Arcipelago. In: Rabassa, J. (ed.), *Late Cenozoic of Patagonia and Tierra del Fuego*. Elsevier, Amsterdam. 227–239.

Isola, I., Bini, M., Ribolini, A., Pappalardo, M., Consoloni, I., Fucks, E., Boretto, G., Ragaini, L. and Zanchetta, G., 2011. Geomorphologic map of northeastern sector of San Jorge Gulf (Chubut, Argentina). *Journal of Maps*, 476–486.

Jouzel, J., Masson-Delmotte, V., Cattani, O., Dreyfus, G., Falourd, S., Hoffmann, G., Minster, B., Nouet, J., Barnola, J.,M., Chappellaz, J., Fischer, H., Gallet, J.C., Johnsen, S., Leuenberger, M., Loulergue, L., Luethi, D., Oerter, H., Parrenin, F., Raisbeck, G., Raynaud, D., Schilt, A., Schwander, J., Selmo, E., Souchez, R., Spahni, R., Stauffer, B., Steffensen, J.P., Stenni, B., Stocker, T.F., Tison, J.L., Werner, M. and Wolff, E.W., 2007. Orbital and millennial Antarctic climate variability over the past 800,000 years. *Science*, 317 (5839), 793–796.

Kaplan, M.R., Strelin, J.A., Schaefer, J.M., Denton, G.H., Finkel, R.C., Schwartz, R., Putnam, A.E., Vandergoes, M.J., Goehring, B.M. and Travis S.G., 2011. In-situ cosmogenic 10Be production rate at Lago Argentino, Patagonia: implications for late glacial climate chronology. *Earth and Planetary Science Letters*, 309 (1–2), 21–32.

Kilian, R. and Lamy, F., 2012. A review of Glacial and Holocene palaeoclimate records from southernmost Patagonia (49–55°S). *Quaternary Sciences Reviews*, 53, 1–23.

Lemieux-Dudon, B., Blayo, E., Petit, J.-R.,Waelbroeck, C., Svensson, A., Ritz, C., Barnola, J.M., Narcisi, B. and Parrenin, F., 2010. Consistent dating for Antarctic and Greenland ice cores. *Quaternary Sciences Reviews*, 29, 8–20.

Markgraf, V. and Huber, U.M., 2010. Late and postglacial vegetation and fire history in Southern Patagonia and Tierra del Fuego. *Paleogeography, Paleoclimatology, Paleoecology*, 297, 351–366.

Moreno, P.M., Kaplan, M.R., François, J.P., Villa-Martinez, R., Moy, C.M., Stern, C.R. and Kubik, P.W., 2009. Renewed glacial activity during the Antarctic Cold Reversal and persistence of cold conditions until 11.5 ka in SW Patagonia. *Geology*, 37, 375–378.

Perez-Alberti, A., Valcarcel Díaz, M., Coronato, A., Rabassa, J. and Costa Casais, M., 2008. Wedge structures

© 2014 Swedish Society for Anthropology and Geography

in southernmost Argentina (Río Grande, Tierra del Fuego). *Ninth International Conference on Permafrost*, Fairbanks, University of Alaska, Alaska. 1381–1385.

Putnam, A., Schaefer, J., Barrell, D.J.A., Vandergoes, M., Denton, G.H., Kaplan, M., Finkel, R.C., Schwartz, R., Goehring, B.M. and Kelley, S., 2010. In situ cosmogenic 10Be production-rate calibration from the Southern Alps, New Zealand. *Quaternary Geochronology*, 5, 392–409.

Reimer, P.J., Baillie, M.G.L., Bard, E., Bayliss, A., Beck, J.W., Blackwell, P.G., Bronk Ramsey, C., Buck, C.E., Burr, G.S., Edwards, R.L., Friedrich, M., Grootes, P.M., Guilderson, T.P., Hajdas, I., Heaton, T.J, Hogg, A.G., Hughen, K.A., Kaiser, K.F., Kromer, B., McCormac, F.G., Manning, S.W., Reimer, R.W., Richards, D.A., Southon, J.R., Talamo, S., Turney, C.S.M., van der Plicht, J. and Weyhenmeyer, C.E., 2009. IntCal09 and Marine09 radiocarbon age calibration curves, 0–50,000 years cal BP. *Radiocarbon*, 51, 1111–1150.

Ribolini, A., Aguirre, M., Baneschi, I., Consoloni, I., Fuck, E., Isola, I., Mazzarini F., Pappalardo, M., Zanchetta, G. and Bini, M., 2011. Holocene beach ridges and coastal evolution in the Cabo Raso Bay (Atlantic Patagonian Coast, Argentina). *Journal of Coastal Research*, 27, 973–983.

Rutter, N., Schnack, E.J., Fasano, J.L., Isla, F.I., del Rio, J., Radtke, U., 1989. Correlation and dating of Quaternary littoral zones along the coast of Patagonia and Tierra del Fuego. *Quaternary Science Reviews*, 8, 213–234.

Schellmann, G., 1998. Jungkänozonische Landschaftsgeschichte patagoniens (Argentinien). Andine Vorlandvergletchenrungen, Talentwicklung und marine Terrassen. *Essener Geographische Arbeiten*, 29. Essen, Germany.

Schellmann, G. and Radtke, U., 2010. Timing and magnitude of Holocene sea-level changes along the middle and south Patagonian Atlantic coast derived from beach ridge systems, littoral terraces and valley-mouth terraces. *Earth-Science Reviews*, 103, 1–30.

Smith, J., Vance, D., Kemp, R.A., Archer, C., Toms, P., King, M. and Zarate, M., 2003. Isotopic constraints on the source of Argentinean loess-with implication for atmospheric circulation and provenance of Antarctic dust during recent glacial maxima. *Earth and Planetary Science Letters*, 212, 181–196.

Stenni, B., Jouzel, J., Masson-Delmotte, V., Röthlisberger, R., Castellano E., Cattani, O., Falourd, S., Johnsen, S.J., Longinelli, A., Sachs, J.P., Selmo, E., Souchez, R., Steffensen, J.P. and Udisti, R., 2004. *Earth and Planetary Science Letters*, 217 (1–2), 183–195.

Sterk, G., Parigiani, J., Cittadini, E., Peters, P., Scholberg, J. and Peri, P., 2012. Aeolian sediment mass fluxes on a sandy soil in Central Patagonia. *Catena*, 95, 112–123.

Stine, S. and Stine, M., 1990. A record form Lake Cardiel of climate change in southern South America. *Nature*, 345, 705–708.

Sun, J.M., Ding, Z.L., Liu, T.S., Rokosh, D. and Rutter, N., 1999. 580,000-Year environmental reconstruction from aeolian deposits at the Mu Us Desert margin, China. *Quaternary Science Reviews*, 18, 1351–1364.

Sun, J.M., Li, S.H., Han, P. and Chen, Y.Y., 2006. Holocene environmental changes in the central Inner Mongolia, based on single-aliquot-quartz optical dating and multiproxy study of dune sands. *Palaeogeography, Palaeoclimatology, Palaeoecology*, 233, 51–62.

Svensson, H., 1988. Ice-wedge casts and relict polygonal patterns in Scandinavia. *Journal of Quaternary Science*, 3, 57–67.

Sylwan, C.A., 2001. Geology of the Golfo San Jorge Basin, Argentina. Geología de la Cuenca del Golfo San Jorge, Argentina. *Journal of Ibarian Geology*, 27, 123–157.

Terrasi, F., De Cesare, N., D'Onofrio, A, Lubritto, C., Marzaioli, F., Passariello, I., Rogalla, D., Sabbarese, C., Borriello, G., Casa, C. and Palmieri, A., 2008. High precision 14C AMS at CIRCE. *Nuclear Instruments and Methods in Physics Research*, B 266 (10), 2221–2224.

Trombotto, D., 2002. Inventory of fossil cryogenic forms and structures in Patagonia and the mountains of Argentina beyond the Andes. *South American Journal of Earth Sciences*, 98, 171–180.

Vogt, T. and del Valle, H.F., 1994. Calcretes and cryogenic structures in the area of Puerto Madryn (Chubut, Patagonia, Argentina). *Geografiska Annaler: Series A, Physical Geography*, 76A, 57–75.

Whalley, W.B. and Langway, C.C., 1980. A scanning electron microscope examination of subglacial quartz grains from Camp Century Core, Greenland – a preliminary study. *Journal of Glaciology*, 25, 91, 125–132.

Woronko, B. and Hoch, M., 2011. The development of frost-weathering microstructures on sand-sized quartz grains: examples from Poland and Mongolia. *Permafrost and Periglacial Processes*, 22, 214–227.

Wang, Y., Amudson, R. and Trumbore, S., 1994. A model of $^{14}CO^2$ and its implications for using 14C to date pedogenic carbonate. *Geochimica et Cosmochimica Acta*, 58, 393–399.

Wright, J., Smith, B. and Whalley, B., 1998. Mechanism of loess-sized quartz silt production and their relative effectiveness: laboratory simulations. *Geomorphology*, 23, 15–34

Zanchetta, G., Bini, M., Isola, I., Pappalardo, M., Ribolini, A., Consoloni, I., Boretto, G., Fucks, E., Ragaini, L. and Terrasi, F., 2014. Middle- to late-Holocene relative sea-level changes at Puerto Deseado (Patagonia, Argentina). *The Holocene*, 29 January. doi: 10.1177/0959683613518589

Zanchetta, G., Consoloni, I., Isola, I., Pappalardo, M., Ribolini A., Aguirre, M., Fucks E., Baneschi, I., Bini, M., Mazzarini, F., Ragaini, L. and Terrasi, F., 2012. New insight on the Holocene marine transgression in the Bahia Camarones (Chubut, Argentina). *Italian Journal of Geosciences*, 131, 19–31.

Zarate, M.A., 2003. Loess of southern South America. *Quaternary Sciences Reviews*, 22, 1987–2006.

Manuscript received 8 Mar., 2013; revised and accepted 30 Dec., 2013

Supporting information

Additional Supporting Information may be found in the online version of this article at the publisher's web-site:

© 2014 Swedish Society for Anthropology and Geography

Fig. S1. Optical Stimulated Luminescence analysis. Equivalent dose as a function of preheat temperature for sample a) WP301B and b) WP301C. The cut-heat temperature was 40°C lower than the preheat temperature. Three aliquots were used per preheat temperature and the error bars represent 1SD. Dose recovery test as a function of preheat temperature for sample c) WP301B and d) WP301C. The cut-heat temperature was 40°C lower than the preheat temperature. Three aliquots were used per preheat temperature and the error bars represent 1SD. SAR growth curve obtained for sample WP301B (e, f). The De is obtained by interpolating the corrected natural signal on the growth curve Repeated dose point (recycling) and zero dose point (recuperation) are reported (e). Histogram summarizing the De distribution for sample WP301B (f).

© 2014 Swedish Society for Anthropology and Geography